JACC Vol. 22, No.2
August 1993:535-41

Automated Flow Rate Calculations Based on Digital Analysis of Flow Convergence Proximal to Regurgitant Orifices

PIETER M. VANDERVOORT, MD,* DAVID H. THOREAU, MBBS, J. MIGUEL RIVERA, MD,*
ROBERT A. LEVINE, MD, FACC, ARTHUR E. WEYMAN, MD, FACC,
JAMES D. THOMAS, MD, FACC*

Boston, Massachusetts and Cleveland, Ohio

Objectives. **The purpose of the study was to develop and validate an automated method for calculating regurgitant flow rate using color Doppler echocardiography.**

Background. **The proximal flow convergence method is a promising approach to quantitate valvular regurgitation noninvasively because it allows one to calculate regurgitant flow rate and regurgitant orifice area; however, defining the location of the regurgitant orifice is often difficult and can lead to significant error in the calculated flow rates. To overcome this problem we developed an automated algorithm to locate the orifice and calculate flow rate based on the digital Doppler velocity map.**

Methods. **This algorithm compares the observed velocities with the anticipated relative velocities, cos $\varphi/2\pi r^2$. The orifice is localized as the point with maximal correlation between predicted and observed velocity, whereas flow rate is specified as the slope of the regression line. We validated this algorithm in an in vitro model for flow through circular orifices with planar surroundings and a porcine bioprosthesis.**

Results. **For flow through circular orifices, flow rates calculated on individual Doppler maps and on an average of eight velocity maps showed excellent agreement with true flow, with $r = 0.977$ and $\Delta Q = -3.7 \pm 15.8$ cm^3/s and $r = 0.991$ and $\Delta Q = -4.3 \pm 8.5$ cm^3/s, respectively. Calculated flow rates through the bioprosthesis correlated well but underestimated true flow, with $r = 0.97$, $\Delta Q = -10.9 \pm 12.5$ cm^3/s, suggesting flow convergence over an angle $>2\pi$. This systematic underestimation was corrected by assuming an effective convergence angle of 212°.**

Conclusions. **This algorithm accurately locates the regurgitant orifice and calculates regurgitant flow rate for circular orifices with planar surroundings. Automated analysis of the proximal flow field is also applicable to more physiologic surfaces surrounding the regurgitant orifice; however, the convergence angle should be adjusted. This automated algorithm should make quantification of regurgitant flow rate and regurgitant orifice area more reproducible and readily available in clinical cardiology practice.**

(J Am Coll Cardiol 1993;22:535–41)

A more accurate assessment of valvular incompetence remains an important goal in clinical cardiology. Currently, regurgitant lesions are predominantly assessed in a semiquantitative manner on the basis of the extent and intensity of contrast in the receiving chamber by ventriculography or aortography (1–3) or simple measurements of height, length or area of the regurgitant jet by Doppler color flow mapping (4–6). Recently, two new quantitative approaches were proposed to assess valvular regurgitation noninvasively using Doppler echocardiography: the momentum technique (7,8) and the proximal flow convergence method (9,10). Of these two methods, the proximal flow convergence method appears to be a promising technique in left-sided regurgitation and has been validated numerically, experimentally and clinically (11,12).

The principle of conservation of mass dictates that flow approaches a regurgitant orifice as a series of concentric shells with decreasing surface area and increasing velocity. Flow rate can then be calculated at any of these isotachs as the surface area of the shell multiplied by its corresponding velocity. The usual implementation of this method is to measure the radius r from the regurgitant orifice to an isovelocity contour displayed as a red-to-blue aliasing border in the color Doppler display. The corresponding velocity v_a of that aliasing contour can be read out from the color calibration bar. Flow rate Q can then be calculated as $Q = 2\pi r^2 v_a$, assuming hemispheric symmetry of the proximal flow field. This assumption is strictly valid only for inviscid flow approaching a point orifice; however, simple correction factors have been proposed to apply this principle to more complex local and global geometries (11,13).

Currently, the radius from the orifice to the isovelocity contour is manually measured from the color-coded velocity maps displayed on a video monitor. This approach may lead to potential errors of two sorts: 1) the localization of the regurgitant orifice is often difficult, and small errors in radius

From the Noninvasive Cardiac Laboratory, Massachusetts General Hospital and Harvard Medical School, Boston, Massachusetts and the *Department of Cardiology, Cleveland Clinic Foundation, Cleveland, Ohio. Dr. Thomas is supported in part by the Bayer Fund for Cardiovascular Research, New York, New York.

Manuscript received October 2, 1992; revised manuscript received February 8, 1993, accepted February 9, 1993.

Address for correspondence: James D. Thomas, MD, Department of Cardiology, Desk F15, Cleveland Clinic Foundation, 9500 Euclid Avenue, Cleveland, Ohio 44195.

0735-1097/93/$6.00

JACC Vol. 22, No.2
August 1993:535-41

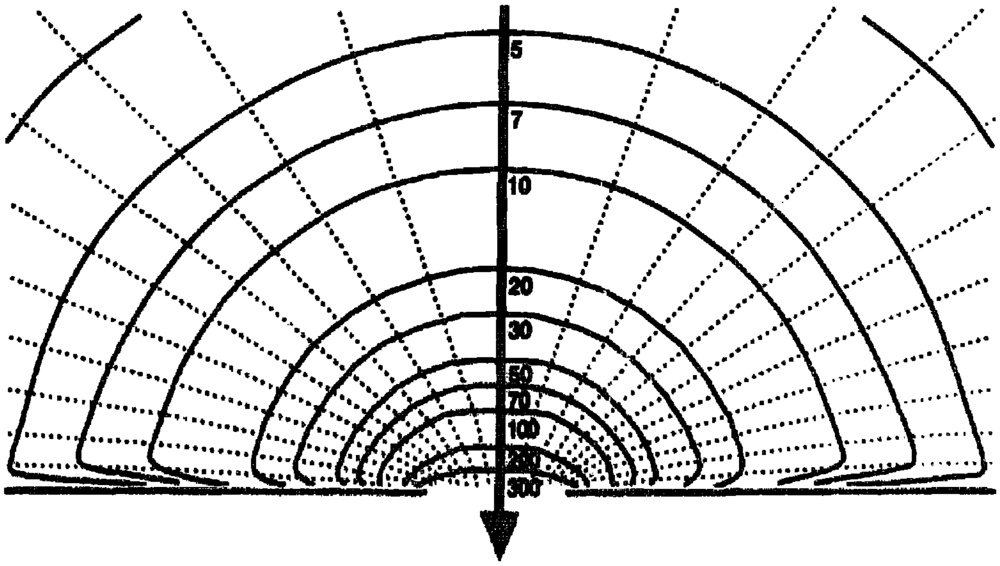

Figure 1. Diagram of flow converging toward a finite orifice (located at the bottom), showing the streamlines (dotted lines) and the consecutive isovelocity contours (solid lines). The velocities of each contour are expressed in cm/s and correspond to $176\text{-cm}^3/\text{s}$ flow rate through an 8-mm diameter orifice.

measurements may result in significant errors in the subsequent flow calculations; and 2) analysis of a single point at a single isovelocity contour wastes most of the information available in the velocity maps and is prone to random errors. To overcome these problems, we developed an algorithm that automatically defines the orifice location and calculates the regurgitant flow rate using the full velocity map of the converging flow field, output in digital format. This method allows automation of the analysis of the converging flow field, which in the future may facilitate more routine clinical application of the proximal flow convergence method in the assessment of valvular incompetence. To further validate this automated algorithm, we performed an in vitro study in which flow rates were calculated for two geometric configurations: 1) circular orifices with planar surroundings; and 2) porcine bioprosthetic valves with central regurgitation.

Methods

Theoretic background. Hydrodynamic theory predicts that inviscid flow approaches an infinitesimal orifice with planar surroundings as a series of concentric hemispheric shells with decreasing surface area and increasing velocity. For flow converging to a circular orifice in a flat surface, the rapid decrease in static pressure approaching the orifice suppresses formation of boundary layers and supports the assumption that these shells are hemispheric in shape (14). In the clinical situation regurgitant orifices are not infinitesimally small but have a finite size. For flow approaching a finite orifice, these isovelocity surfaces have been shown to be roughly hemispheric in shape, but they start to flatten out as they come closer to the orifice (Fig. 1). We assume that in the proximal converging flow field at a distance from the regurgitant orifice, there is a region where the velocity field approximates inviscid flow converging to a pointlike orifice. In this region the velocity distribution will be given by $|v| = Q/2\pi r^2$, where $|v|$ is the velocity magnitude at a distance r from the orifice and Q is the instantaneous orifice flow rate. The velocity displayed by the Doppler instrument will not be the velocity magnitude $|v|$ but the velocity component parallel to the ultrasound beam, or $|v| \cos \varphi$, where φ is the angle between the ultrasound beam and the direction of the flow. Because flow is directed toward the orifice, φ can be calculated for each point in the velocity field when its location relative to the orifice and the ultrasound transducer is known.

Computer algorithm. Using color Doppler imaging, it is possible to obtain a digital map of blood velocity on an ≈0.5-mm grid. The location of the transducer relative to the imaged flow field can easily be determined because its coordinates are stored with the digital velocity maps. To find the regurgitant orifice, the user first specifies a box within which the orifice is expected to lie. Within this box an array of points, representing individual pixels from the digital map, is defined. Each of these points is then tested as a possible orifice center. For each of these test centers, an expected velocity component field is generated as $v \propto \cos \varphi/2\pi r^2$. This generated velocity field is only proportional to the actual velocity field because the flow rate Q is at this point unknown. For each test center, a correlation coefficient is calculated between the generated velocity field and the observed velocity field. The test center with the highest correlation coefficient is chosen as the orifice center. The flow rate is then given by the slope of the line relating the calculated velocities $\cos \varphi/2\pi r^2$ with the actual velocity components v.

The entire proximal flow convergence zone is not analyzed because correlation coefficients can be calculated between predicted and observed velocity only in regions where velocities are reliably displayed on the Doppler color flow map. Figure 2 shows the different regions that must be excluded from analysis. First, in the immediate vicinity of the orifice, velocity increases above the Nyquist velocity and may alias several times, specifically in left-sided lesions

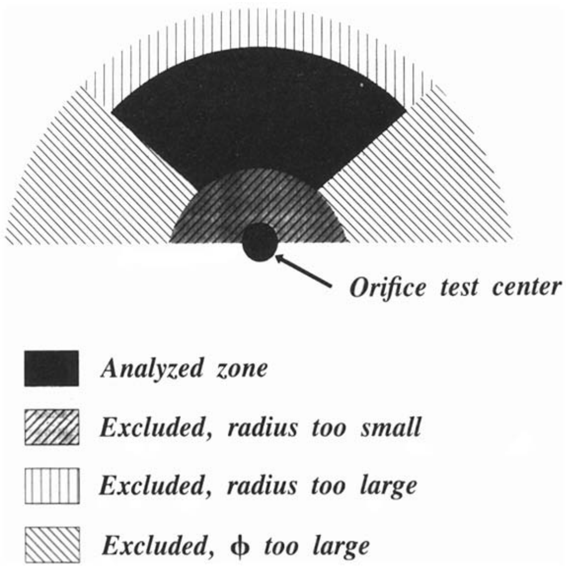

Figure 2. Schematic display of a proximal flow convergence zone, showing the zone that is analyzed and the different zones excluded from analysis by the automated algorithm. ϕ = angle between direction of flow and ultrasound beam.

where the orifice velocities are high. Also, close to the orifice the isovelocity contours flatten out (Fig. 1), and the hemispheric assumption implicit in the $1/r^2$ relation no longer holds (11). Second, far from the orifice, velocities are very low, and relatively small flow fluctuations, additional flow fields and the coarse velocity quantitation of Doppler color flow mapping (typically 5 bits, or 1 part in 32 resolution) can introduce significant errors into the flow calculations. In the initial implementation of this algorithm, the inner and outer borders of the region selected for analysis were specified manually on the digital maps. Finally, regions >45° off the central axis have such a high value for φ that the signal to noise ratio within the Doppler velocity field becomes unacceptable.

In vitro experiment. For this study we used a previously described in vitro flow model to generate steady state flow through circular orifices with planar surroundings and orifice area ranging from 0.1 to 1.0 cm^2 (8). A 1% to 2% aqueous solution of cornstarch provided acoustic reflectors. By changing the pressure in the proximal chamber, the flow rates were varied between 13 and 246 cm^3/s. A total of 41 different hydrodynamic conditions were studied.

To simulate a more clinically relevant surrounding geometry, a porcine bioprosthetic valve (21 mm, Hancock Extracorporeal Medical Specialties) was mounted in the septum dividing the proximal and distal chamber of the flow model. Different sizes of circular tubing were fixed between the leaflet tips, preserving the global leaflet geometry of the valve, simulating central valvular regurgitaion due to prosthetic degeneration. Seven different hydrodynamic stages were studied with flow rates ranging from 11 to 129 cm^3/s.

Echocardiographic data. Doppler color flow images of the converging flow field were obtained using an Ultramark 9 (Advanced Technology Laboratories) equipped with a digital dataport. A 2.25-MHz phased array transducer was positioned along the central axis of the flow. The color gain was adjusted to avoid artifactual color noise. The largest packet size (number of pulses averaged per scan line) and the lowest available wall filter were used (15). All color flow images were obtained at a pulse repetition frequency of 1,250 Hz. For one hydrodynamic stage we varied the pulse repetition frequency from 450 to 4,000 Hz while keeping the flow rate constant. By changing the pulse repetition frequency (and thus the Nyquist velocity), the range of uniquely displayed velocities available for flow calculations in the converging flow field was varied, and its effect on the calculated flow rates using the automated algorithm was analyzed.

To evaluate in more detail the effect of the surrounding geometry on calculated flow rates in the porcine bioprosthetic valve, the proximal flow convergence zone was imaged in two orthogonal planes for each hydrodynamic stage.

Data analysis. Digital velocity maps of selected freezeframes were transferred to a personal computer for analysis. Velocity data (5 bits) and variance data (3 bits) were output in polar coordinate format, typically 256 points along each of the 64 scan lines. These files were analyzed using custom software written in the ASYST scientific programming environment (Keithley-Asyst). As previously explained, a rough region of interest was specified, within which the orifice was expected to lie. All points in this region of interest were tested as possible orifice centers, and the one that showed the best correlation between predicted and actual velocity was chosen to calculate flow rate. The orifice location selected by the computer was compared with the location on a hard copy printout of the original experimental acquisition. To avoid random error in the selection of the color flow maps, eight representative velocity maps were averaged for each hydrodynamic stage. To evaluate the effect of frame-to-frame variability on the calculated flow rates in this steady-state model, flow rates were also calculated on three individual velocity maps throughout a similar range of hydrodynamic conditions.

For flow calculations through the bioprosthesis, five to eight velocity maps were averaged. When the geometric configuration surrounding a regurgitant orifice is nonplanar, the convergence angle (and thus the constant 2π) must be modified. For rudimentary geometric configurations, relatively simple correction factors have been proposed. For an orifice surrounded by a wedge-shaped surface, 2π has to be adjusted in proportion to the solid angle subtended by the two surfaces; for an orifice in a funnel or on top of a cone, the correction factor is $2\pi(1 - \cos \theta)$, where θ is the angle between the direction of the proximal flow and the conal surface (Fig. 3). Although a simplification, these geometric surfaces may represent a reasonable approximation of more

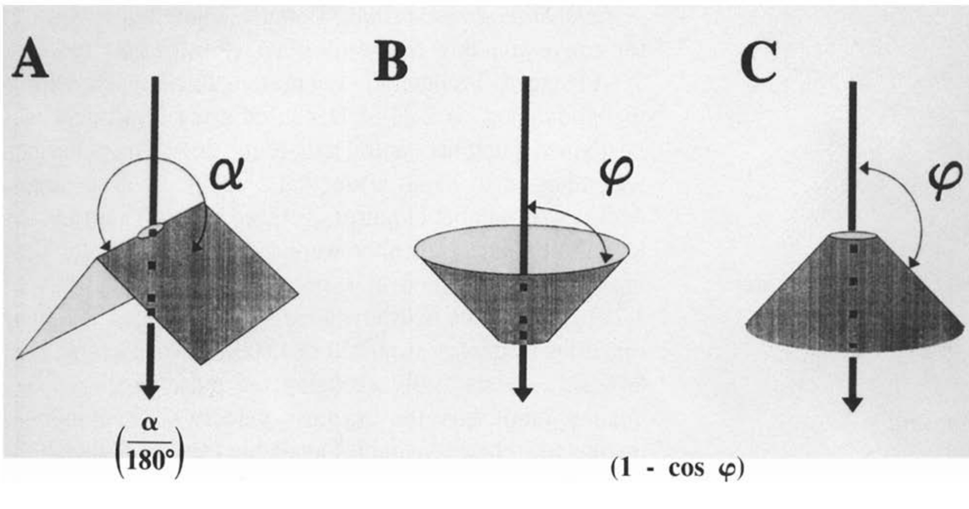

Figure 3. Schematic display of different geometric configurations approximating the leaflet surface surrounding a regurgitant orifice and their respective correction factors to calculate flow by the proximal flow convergence method: **A**, wedge shape; **B**, funnel; **C**, cone. The arrow indicates the direction of the flow. φ = angle between central axis of proximal flow and conal surface; α = solid angle subtended by the two surfaces.

complex clinical situations. To evaluate the effect of the trileaflet prosthetic geometry surrounding the regurgitant orifice on calculated flow rates, the valvular surface was approximated as a cone with the orifice at the top. The effective convergence angle was then determined by comparing actual and calculated flow rates.

Results

A total of 401 Doppler velocity maps were digitally stored and analyzed. The developed algorithm was able to localize the orifice center quite precisely, typically up to 1-mm accuracy. For the selected orifice locations, the observed velocity field correlated well with the theoretically expected $v \propto \cos \varphi/2\pi r^2$ velocity distribution, with r values ranging from 0.84 to 0.99. This correlation peaked sharply as one moved laterally across the region of interest but was less well defined when one moved axially through the field. Figure 4 shows the expected and the actual Doppler velocity component distribution of a proximal flow convergence region. Not only is there a very strong linear correlation between the predicted and observed velocities for the 442 pixels within the analysis zone, but the regression line passes through the origin, as it must if the orifice center has been appropriately localized. As shown here, the flow rate (103 cm^3/s) is closely approximated by the slope of the regression line.

For 25 different flow rates ranging between 23 and 245 cm^3/s, eight Doppler velocity maps were averaged. Calculated flow rates based on the averaged velocity maps showed an excellent correlation with the actual flow rates, with r = 0.991, y = 0.95x + 0.83 and a mean error (calculated minus true flow) of $\Delta Q = -4.3 \pm 8.5$ cm^3/s (Fig. 5).

For a steady flow of 103.3 cm^3/s, the calculated flow rates based on velocity maps obtained with seven different pulse repetition frequencies ranging between 450 and 4,000 Hz showed a mean error (calculated minus true flow) of ΔQ = 1.5 ± 6.6 cm^3/s. Linear regression analysis showed no

Figure 4. Observed velocity components (y axis) plotted against $\cos \phi/2\pi r^2$ (x axis) for 442 pixels in the proximal flow field for a given test orifice center. Estimated flow rate, given by the slope of this line, closely approximates the true flow rate (103.3 cm^3/s).

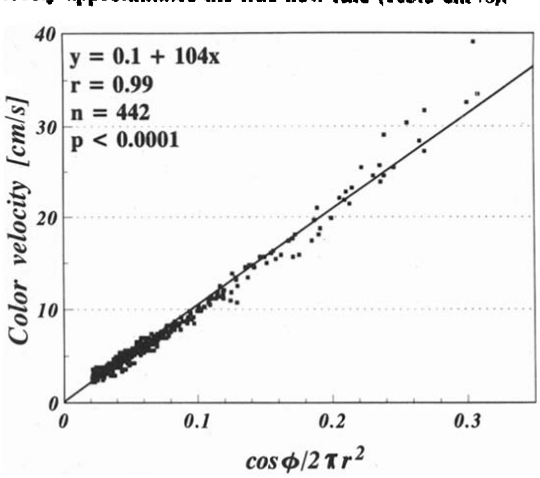

Figure 5. Correlation between the true flow rate (x axis) and the flow rate calculated by the automated algorithm (y axis) for circular orifices with planar surroundings. Eight representative digital Doppler velocity maps were averaged for subsequent flow rate calculations. Δ = calculated minus true flow.

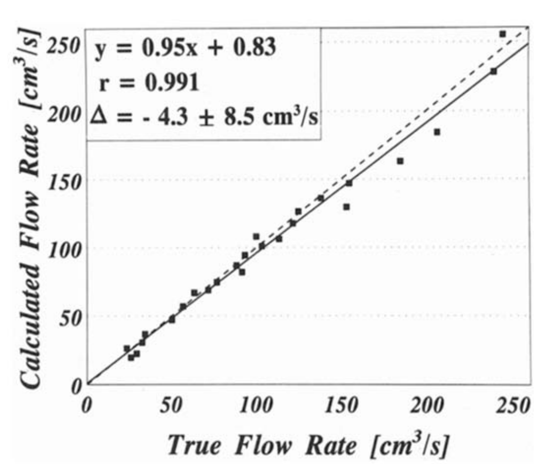

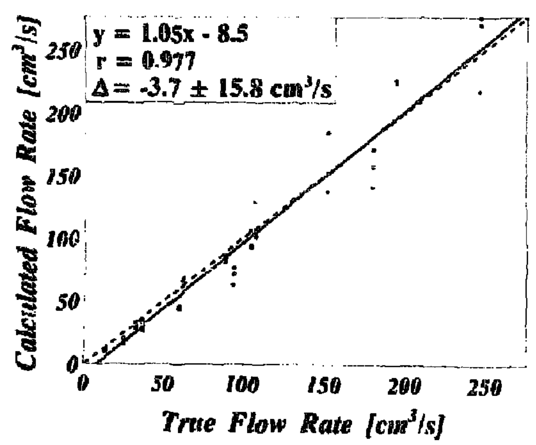

Figure 6. Correlation between the true flow rate (x axis) and the flow rate calculated by the automated algorithm on individual Doppler velocity maps (y axis) for circular orifices with planar surroundings.

significant relation between pulse repetition frequency and the accuracy of calculated flow rates ($p > 0.05$).

For 14 different hydrodynamic stages with flow rates ranging between 13 and 246 cm^3/s, flow rates were calculated for individual (rather than averaged) Doppler velocity maps. Calculated flow rates still agreed well with true flow rates, with $r = 0.977$, $y = 1.05x - 8.5$ and a mean error (calculated minus true flow) of $\Delta Q = -3.7 \pm 15.8$ cm^3/s (Fig. 6).

For flow rate calculations through the porcine xenograft, five to eight Doppler velocity maps were averaged. For each hydrodynamic stage, flow rates were calculated for two orthogonal scanning positions, assuming flow convergence over 2π. The flow rates obtained from two orthogonal views were not significantly different, and individual values are shown in Figure 7. The mean flow rate from the two orthogonal scanning positions was calculated for each stage, and it correlated quite well with the actual flow rates ($r = 0.97$); however, true flow (x) was underestimated, with $y = 0.83x - 1.45$ and a mean error (calculated minus true flow) of $\Delta Q = -10.9 \pm 12.5$ cm^3/s. This underestimation indicated that flow was converging on the orifice over an angle >180°. Assuming a convergence funnel of 212° ($\theta = 106°$, $1 - \cos \theta = 1.276$) almost completely corrected the systematic underestimation, with $\Delta Q = 0.5 \pm 12.2$ cm^3/s.

Figure 7. Correlation between the true flow rate (x) and the flow rate calculated by the automated algorithm (y) in the porcine xenograft. **Small squares** = individual flow rate calculations in two orthogonal views, assuming flow convergence over 2π; **large squares** = mean flow rates of the two orthogonal views; **triangles** = calculated flow rates after correction for the surrounding geometric configuration.

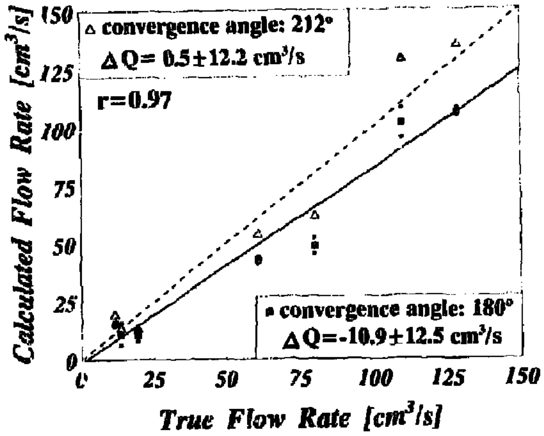

Discussion

Analysis of the proximal flow convergence zone appears to be a promising approach to quantify valvular incompetence noninvasively using Doppler color flow mapping. This method not only allows the calculation of regurgitant flow rate through incompetent valves (12), but also permits one to estimate the effective regurgitant orifice area, a variable that provides unique information on the fundamental incompetence of regurgitant valves, largely independent of hemodynamic conditions (16,17).

It has been shown that flow approaches a restrictive orifice as a series of roughly hemispheric shells and that flow rate can be calculated as $Q = 2\pi r^2 v$. This concept has been validated numerically and experimentally with two general exceptions: 1) close to the orifice where the isovelocity surfaces flatten out and the hemispheric assumption no longer holds; and 2) when the regurgitant orifice lies in a nonplanar structure, the constant 2π has to be adjusted for the surrounding geometry, and relatively simple correction factors have been proposed (11,13).

As currently implemented, however, flow rates are calculated on the basis of radius measurements of a single isovelocity contour. Particularly in clinical applications, it is often difficult to localize the regurgitant orifice, which may lead to significant errors in the calculated flow rates. To overcome some of these limitations, we developed an automated algorithm to calculate flow rates based on the digital Doppler velocity maps. The proposed algorithm offers several potential advantages over current analysis of the proximal flow convergence zone. It is less dependent on operator intervention (such as baseline shifting of the color bar to highlight a single isovelocity contour) because it uses the entire velocity map of the converging flow field. Furthermore, by comparing the actual velocity field with a theoretically predicted velocity distribution, the algorithm will allow one to localize the effective regurgitant orifice and subsequently calculate regurgitant flow rate and effective regurgitant orifice area.

Results of the current study. The close correlations observed between the predicted and the actual velocity fields (Fig. 4) confirm the assumption that the flow field at a distance from a finite orifice approximates a hemispheric flow field converging to an infinitesimal orifice. On the basis of this assumption, the automated algorithm is able to localize the regurgitant orifice quite accurately, as verified by direct comparison of the computer-selected orifice location with hard copy printouts of the experimental setup. The accuracy of the selected orifice location is also reflected by the regression line relating the predicted and observed velocity fields, which passes through the origin, as it should when the regurgitant orifice is appropriately localized. The slope of this regression line yields the regurgitant flow rate and shows excellent agreement with the true flow ($r = 0.991$ and $\Delta Q = -4.3 \pm 8.5$ cm^3/s) throughout a range of clinically relevant driving pressures and flow rates. Varying the velocity range (by varying pulse repetition frequency) in the proximal flow field available for analysis did not affect the flow rate calculations significantly. In clinical applications analysis of the proximal flow convergence is performed on single Doppler color flow images; therefore the algorithm was also applied to individual Doppler velocity maps. Throughout a similar range of hydrodynamic conditions, the flow rates calculated on single-velocity maps correlated closely with the actual flow rates ($r = 0.977$ and $\Delta Q = -3.7 \pm 15.8$ cm^3/s). The variation of the calculated flow rates is slightly higher because of the frame to frame variability of the Doppler color flow maps; however, the overall accuracy remains very good.

We also tried this algorithm in more physiologic regurgitant orifices, which lie in nonplanar surroundings. To investigate this situation we studied regurgitation through a porcine xenograft. The calculated flow rates (y) correlated well with the true flow rate (x) ($r = 0.97$, $y = 0.83x - 1.45$); however, true flow was underestimated by $\Delta Q = -10.9 \pm 12.5$ cm^3/s, indicating that flow converges over >180°. The geometry of the three bioprosthetic leaflets surrounding the regurgitant orifice was approximated as a cone with the regurgitant orifice at the top. A flow convergence angle of 212° corrected the underestimation, with $\Delta Q = 0.5 \pm 12.2$ cm^3/s.

Limitations and future directions. As currently implemented, the inner and outer borders of the analyzed zone in the proximal flow convergence, selected to exclude aliased and very low velocities from analysis, have to be specified manually on the digital Doppler velocity maps. In the future, however, it should be possible to eliminate this step of user intervention and have the algorithm select the velocity range to be analyzed automatically. In general, it appears that velocities between ≈20% and 150% of the Nyquist velocity give the most robust flow estimations; radii corresponding to these velocities could be selected automatically by searching inward from the periphery of the convergence zone toward the tested orifice center.

The algorithm calculates flow rates as $Q = 2\pi r^2 v$, assuming hemispheric flow convergence over 180°. This assumption may not be correct in clinical practice because orifice geometry and surface geometry will affect the shape of the converging flow field. Previous studies, as well as our data, suggest that the convergence angle should be adjusted to correspond to the surrounding geometric configuration. Physiologic valve surfaces are very complex structures surrounding the regurgitant orifice; however, they can be approximated by relatively simple geometric structures, and correction factors have been proposed to adjust for wedge-shaped or conal geometries. Before this automated algorithm can be used routinely in a clinical setting to evaluate regurgitation, the effect of valve geometry on the converging flow field needs to be evaluated in more detail. As a first step, we studied the effect of the surrounding geometric configuration in a trileaflet bioprosthetic valve on the calculated flow rates and demonstrated that the convergence angle needs to be adjusted; however, correction factors for clinical situations remain to be determined and may be different for different types of valves. It is hoped that a reasonable estimate of convergence angle can be obtained from observation of the geometry from two-dimensional sector scanning. This automated algorithm can be applied to Doppler flow maps obtained by transthoracic or transesophageal imaging. Once clinically validated, it will allow the study of in vivo effects of eccentric regurgitant orifices, proximal chamber constraint or the presence of a flail leaflet. Particularly with leaflet flail, the distorted valve geometry may significantly affect the proximal flow field and thus the calculated flow rates, as shown by some preliminary computational fluid dynamics simulations (18).

In the current study we validated the automated algorithm in steady flow conditions. Although the concept of conservation of mass is preserved under pulsatile flow conditions at each point in time (for incompressible fluid), the limited temporal resolution of two-dimensional Doppler color flow mapping may introduce an error into the calculated flow rates. Particularly at faster heart rates it may not be possible to resolve the maximal instantaneous flow rate, and this may lead to underestimation of regurgitant stroke volume and regurgitant flow rate.

Conclusions. The developed algorithm for automated flow rate calculations proved to be accurate and reproducible for flow approaching circular orifices with planar surroundings in the controlled environment of an in vitro setting. Automated analysis of the converging flow field is also applicable to more physiologic nonplanar surfaces surrounding the regurgitant orifice. When validated clinically, this algorithm could be incorporated in the calculation package of contemporary echocardiographs, which should make quantification of regurgitant flow rate and regurgitant orifice area easier, more reproducible and more readily available for clinical cardiology practice.

References

1. Nagle RE, Walker D, Grainger RG. The angiographic assessment of mitral incompetence. Clin Radiol 1968;19:154–64.
2. Baron MG. Angiographic evaluation of valvular insufficiency. Circulation 1971;43:599–605.
3. Croft CH, Lipscomb K, Mathis K. Limitations of qualitative angiographic grading in aortic or mitral regurgitation. Am J Cardiol 1984;53:1593–8.
4. Miyatake K, Izumi S, Okamoto M, et al. Semiquantitative grading of severity of mitral regurgitation by real-time two-dimensional Doppler flow imaging technique. J Am Coll Cardiol 1986;7:82–8.

5. Helmcke F, Nanda NC, Hsuin MC, et al. Color Doppler assessment of mitral regurgitation with orthogonal planes. Circulation 1987;75:175–83.
6. Spain MG, Smith MD, Grayburn PA, Harlamert EA, DeMaria AN. Quantitative assessment of mitral regurgitation by Doppler color flow imaging: angiographic and hemodynamic correlations. J Am Coll Cardiol 1989;13:585–90.
7. Cape EG, Yoganathan AP, Levine RA. A new method for noninvasive quantification of valvular regurgitation based on conservation of momentum: an in vitro validation. Circulation 1989;79:1343–53.
8. Thomas JD, Liu CM, Flachskampf FA, O'Shea JP, Davidoff R, Weyman AE. Quantification of jet flow by momentum analysis: an in vitro color Doppler flow study. Circulation 1990;81:247–59.
9. Recusani F, Bargiggia GS, Yoganathan AP, et al. A new method for quantification of regurgitant flow rate using color Doppler flow imaging of the flow convergence region proximal to a discrete orifice: an in vitro study. Circulation 1991;83:594–604.
10. Bargiggia GS, Tronconi L, Sahn DJ, et al. A new method for quantitation of mitral regurgitation based on color flow Doppler imaging of flow convergence proximal to regurgitant orifice. Circulation 1991;84:1481–9.
11. Rodriguez L, Anconina J, Flachskampf FA, Weyman AE, Levine RA, Thomas JD. Influence of flow rate, orifice size and aliasing velocity on flow calculation using the flow convergence method. Circ Res 1992;70:923–30.
12. Rivera JM, Vandervoort PM, Thoreau DH, Levine RA, Weyman AE, Thomas JD. Quantification of mitral regurgitation using the proximal flow convergence method: a clinical study. Am Heart J 1992;124:1289–96.
13. Levine RA, Rodriguez L, Cape EG, et al. The proximal flow convergence method for calculating orifice flow rate requires correction for surrounding leaflet geometry (abstr). J Am Coll Cardiol 1991;17:359.
14. Tritton DJ. Physical Fluid Dynamics. Oxford: Clarendon Press, 1988: 126–7, 283.
15. Vandervoort PM, Thoreau DH, Weyman AE, Thomas JD. Wall filtering significantly increases Doppler velocities in proximal flow convergence (abstr). Circulation 1991;84(suppl II):II-104.
16. Vandervoort PM, Rivera JM, Thoreau DH, Mele D, Weyman AE, Thomas JD. Application of color Doppler flow imaging to calculate effective regurgitant orifice area: an assessment of valvular incompetence independent of hemodynamics (abstr). J Am Coll Cardiol 1992;19:297A.
17. Rivera JM, Vandervoort PM, Thoreau DH, et al. Regurgitant orifice area, a fundamental measure of mitral incompetence: calculation by proximal acceleration (abstr). J Am Coll Cardiol 1992;19:379A.
18. Thomas JD, Powell KA, Greenberg NL, Vandervoort PM, Stewart WJ. Use of the proximal flow convergence method to quantitate mitral regurgitation in patients with a flail leaflet: lessons from fluid dynamical modelling (abstr). J Am Coll Cardiol 1993;21:485A.